Toxicology in Vitro 61 (2019) 104655

Contents lists available at ScienceDirect

Toxicology in Vitro

journal homepage: www.elsevier.com/locate/toxinvit

Chlorpyrifos-induced dysfunction of lipid metabolism is not restored by supplementation of polyunsaturated fatty acids EPA and ARA in Atlantic salmon liver cells

P.A. Olsvik[a,b,*], S.K. Hammer[b], M. Sanden[b], L. Søfteland[b]

[a] Faculty of Biosciences and Aquaculture, Nord University, Bodø, Norway
[b] Institute of Marine Research (IMR), Bergen, Norway

ARTICLE INFO

Keywords:
Agricultural pesticides
Chlorpyrifos
PUFAs
Atlantic salmon
Steatosis
Monoacylglycerol

ABSTRACT

Exposure to contaminants can lead to accumulation of lipids in the liver. This study aimed to examine whether eicosapentaenoic acid (EPA) and arachidonic acid (ARA) supplementation can protect fish cells against the negative impact of chlorpyrifos (CPF). Atlantic salmon hepatocytes were exposed to either 100 μM CPF, 200 μM EPA, 200 μM ARA, or combinations of these for 48 h, and endpoints included lipid droplet formation, gene expression, and global metabolomic analysis. The results showed that polyunsaturated fatty acid (PUFA) supplementation modified the cell lipid composition, reduced uptake of CPF and increased the cellular number and size of lipid droplets. CPF exposure induced the transcription of *ppara* and *fabp3*, and reduced the levels of several PUFAs, and lead to accumulation of monoacylglycerols (MAGs) in the cells. Supplementation of EPA or ARA did not prevent CPF-induced accumulation of MAGs and only to a limited degree rescued the response on other lipids. CPF exposure further reduced energy metabolism, a response partly restored by PUFA supplementation. Reduced levels of glutathione indicated oxidative stress; an effect not ameliorated by the PUFAs. Altogether, this study shows that PUFA supplementation only modestly protects Atlantic salmon hepatocytes against the negative impact of CPF.

1. Introduction

Accumulating evidence suggests that exposure to persistent organic pollutants (POPs) is associated with accumulation of fat in the liver (Grun and Blumberg, 2007; Al-Eryani et al., 2015; Darbre, 2017). Endocrine-disrupting chemicals in particular are linked to fatty liver, due to their ability to bind to and interfere with nuclear receptors (Foulds et al., 2017). Fatty liver occurs when hepatic uptake and/or *de novo* synthesis of free fatty acids exceeds their oxidation and secretion as triglycerides (TAGs) (Foulds et al., 2017). Abnormal accumulation of lipids in the liver has been proposed to be among the most common pathologic hepatic responses to chemical exposure (Cave et al., 2011). In hepatic steatosis, excess TAG is usually stored in lipid droplets sized between 50 nm and 1 μm within the hepatocyte (Sahini and Borlak, 2014). The number and size of lipid droplets, typically present in the cytosol, are well-established histological biomarkers of fatty liver (Willebrords et al., 2015). Excessive synthesis and accumulation of TAG is not necessarily hepatotoxic, but imbalance of free fatty acid metabolism in the hepatocytes may lead to hepatocellular damage, often by initiating a pro-inflammatory cascade (Foulds et al., 2017). Fish studies indicate that the mechanisms underlying the development of fatty liver are conserved across phyla (Zang et al., 2018). In zebrafish (*Danio rerio*), it has been shown that excess nutrients cause increased plasma TAG and hepatic steatosis (Oka et al., 2010). In Atlantic salmon (*Salmo salar*), liver TAG accumulation has been associated with excessive intake of *n*-6 fatty acids due to replacement of marine ingredients with plant ingredients in the diet (Torstensen et al., 2011; Alvheim et al., 2013; Sanden et al., 2016).

Interestingly, some *n*-3 polyunsaturated fatty acids (PUFAs) with anti-inflammatory properties, such as eicosapentaenoic acid (EPA), docosahexaenoic acid (DHA) and α-linolenic acid (ALA), seem to reduce the degree of fat accumulation in the liver. For example, supplementation of EPA can inhibit hepatic steatosis in obese mice (Inoue-Yamauchi et al., 2018). Similar findings have been reported for fish. High levels of the DHA and EPA in the diet protect against nutrient-derived induction of fatty liver in Atlantic salmon (Liland et al., 2013, 2015). Other *n*-6 PUFAs can have the opposite effects, and act pro-inflammatory. Arachidonic acid (ARA) is metabolized to both pro-

* Corresponding author.
E-mail address: pal.a.olsvik@nord.no (P.A. Olsvik).

https://doi.org/10.1016/j.tiv.2019.104655
Received 1 July 2019; Received in revised form 6 September 2019; Accepted 15 September 2019
Available online 16 September 2019

inflammatory and anti-inflammatory eicosanoids. For example, ARA-derived metabolites of the cyclooxygenase (COX) pathway are generally considered to be pro-inflammatory (Cranmer-Byng et al., 2015). ARA may also enhance oxidative stress by non-enzymatic free radical-initiated peroxidation reactions (Vigor et al., 2014). In Atlantic salmon hepatocytes, we have previously shown that while EPA can help protect cells against the negative effects of contaminants, ARA contrarily seems to strengthen the contaminant-induced response (Søfteland et al., 2016). Enhanced protection against contaminant damage has also been demonstrated in rainbow trout (*Oncorhynchus mykiss*) liver cells after PUFA supplementation (Ferain et al., 2016).

In a series of examinations, we have been studying the potential toxicity of agricultural pesticides found in aquafeeds on Atlantic salmon. Sustainable aquafeeds used today contain higher levels of plant ingredients, with more of the *n*-6 ARA precursor linoleic acid (LA) and less *n*-3 EPA and DHA, compared to earlier feeds for salmon that consisted primarily of marine ingredients. These studies have focused on the organophosphorus pesticides (OPs) chlorpyrifos (CPF), chlorpyrifos-methyl (CPM) and pirimiphos-methyl (PPM) (Olsvik et al., 2015, 2017, 2019a; Søfteland et al., 2016; Sanden et al., 2018). One of the main effects of OPs in salmon, both after short-term *in vitro* exposure and after longer-term *in vivo* exposure, is the disruption of lipid metabolism (Søfteland et al., 2016; Sanden et al., 2018). Exposure to OPs typically leads to depletion of long-chain fatty acids and PUFAs, and accumulation of monoacylglycerols (MAGs). Pathway analysis often points to mechanisms linked to accumulation of lipids and steatosis as the main disease and function. Compared to POPs, OPs are more easily biodegraded, and less is known about how these chemicals interfere with lipid metabolism in fish.

In light of this, the aim of this study was to examine to which degree EPA supplementation protects cells against CPF-induced disruption of lipid metabolism, and whether ARA co-supplementation interfere with the potential protective effect of EPA in Atlantic salmon hepatocytes. Other mechanisms potentially impacted by PUFA supplementation, such as detoxification and oxidative stress, were also studied.

2. Material and methods

2.1. In vitro exposure experiment

Hepatocytes were isolated from male Atlantic salmon ($n = 6$, 669 ± 141 g, mean ± st.dev.) with a two-step perfusion method as previously described by Søfteland et al. (2009). After isolation, cell viability was evaluated with the Trypan Blue (Lonzo, Medprobe, Oslo, Norway) exclusion method. Prior to exposure, the cells were cultured for 36–40 h in L-15 medium containing 10% salmon serum (Nordic BioSite, Oslo, Norway), with change of medium after 18–20 h. The cell suspensions were plated on laminin-coated (5 μg/cm^2) plates and chamber slides. Cells were exposed in 6-well plates for metabolomics, in 12-well plates for gene expression analysis (RT-qPCR), and in 96-well plates for cytotoxicity determination (MTT and xCELLigence). Quantification of lipid accumulation with the Oil Red O colorimetric assay was done in 96-well plates, whereas 8-well chamber slides were used for Oil Red O lipid droplet staining. The following cell densities were used; 7.2×10^6 cells per well in 3 mL L-15 medium for metabolomics, 2.6×10^6 cells per well for gene expression analysis, 0.2×10^6 cells per well in 0.2 mL L-15 medium for determination of cytotoxicity and lipid accumulation, and 0.4×10^6 cells per well in 0.5 mL L-15 medium for lipid droplet staining. The L-15 exposure medium, containing 1% salmon serum, was changed after 18–20 h. The number of biological replicates was $n = 6$.

Based on previous work in our laboratory including individual cytotoxicity dose-response curves for CPF and the fatty acids, the hepatocytes were treated with 100 μM CPF, 200 μM of ARA and 200 μM EPA in this study (Søfteland et al., 2016, unpublished work). The treatment 1:1 ratio between ARA and EPA was selected based on earlier *in vitro* studies with salmon hepatocytes using combinations of similar concentrations of ARA and EPA (Søfteland et al., 2016), and *in vivo* studies with salmon (Sissener et al., unpublished work). CPF was dissolved in dimethyl sulfoxide (DMSO) (Scientific and Chemical Supplies Ltd., Bilston, UK). All exposure solutions contained equal amounts of DMSO (0.2%). The fatty acids were purchased from Sigma Chemical Co (St Louis, MO, USA). Binding of fatty acids to fatty acid free-BSA (FAF–BSA) was performed as per Ghioni et al. (1997). To summarize, fatty acids dissolved in 0.04 mL chloroform per mg fatty acid was added to a glass sample tube and N_2 was used to evaporate the chloroform. Potassium hydroxide (KOH) was applied to the fatty acid in a 1:3 ratio and the solution was shaken for 10 min using a vortex mixer. FAF–BSA was employed in a 2.5:1 relationship to the fatty acid and the solution was mixed for 45 min before it was sterile-filtered and preserved at −80 °C in anoxic condition. Unless otherwise noted, chemicals were obtained from Sigma-Aldrich (Oslo, Norway).

2.2. Cytotoxicity screening

Cell viability was determined with the MTT-based *In Vitro* Toxicology assay (Sigma Aldrich). After 48 h of exposure, the cells were incubated with MTT, and the absorbance at 570 nm was determined with an iEMS reader (Labsystems iEMS Reader MF, Helsinki, Finland). The xCELLigence system (Real-Time Cell Analyzer RTCA-SP, ACEA Biosciences, San Diego, USA) was used for impedance-based real-time detection of cell viability (Ke et al., 2011). The data was collected with 2 min intervals for 12 h, and then every 15 min for about 60 h.

2.3. Quantification of lipid droplets and staining of neutral lipids in hepatocytes

For evaluation of the extent of lipid accumulation, the hepatocytes were stained with Oil Red O using a colorimetric assay (Cayman Chemical, Ann Arbor, MI, USA). For quantification of lipid accumulation, 100 μL of the Lipid Droplets Assay Dye Extraction Solution was added to the cells. After gently mixing for 30 min, the samples were transferred to a 96-well plate and the absorbance read at 490 nm with a 96-well plate reader. For histological evaluation of lipid droplet distribution and size, hepatocytes were rinsed with 1xPBS and fixed using 4% paraformaldehyde for 15 min at room temperature. The cells were washed with 1xPBS and air dried, and then stained with Oil Red O for 30 min at room temperature before microscopy examination. Lipid droplets were examined at 20× magnification (Olympus BX51 microscope with UPlanFL N 20× objective, Tokyo, Japan) connected to a CCD camera, using NIS-Elements software.

2.4. RNA isolation and RT-qPCR

The RNeasy Plus mini kit (Qiagen, Crawley, UK) was used to extract total RNA from the hepatocytes. RNA quality was assessed using the NanoDrop ND-1000 UV–Vis Spectrophotometer (NanoDrop Technologies, Wilmington, DE, USA) and the Agilent 2100 Bioanalyzer (Agilent Technologies, Palo Alto, CA, USA). The RNA integrity number (RIN) for 12 randomly selected samples used for gene expression analysis was 9.7 ± 0.1 (mean ± st.dev.).

A two-step real-time RT-qPCR protocol was used to quantify the mRNA levels of 9 target genes and 2 reference genes. Target gene mean normalized expression (MNE) was determined using the geNorm software (Vandesompele et al., 2002) and a normalization factor based upon *rplp0* and *eef1b1* ($M < 0.43$). Supplementary Table S1 shows gene names and PCR assays.

2.5. Protein extraction and western blot

To harvest proteins from cell cultures, the CelLytic M Cell Lysis Reagent was used. Microsomal fractions from the cell lysate were

prepared with differential centrifugation. After centrifugation at 12,000 ×*g* for 20 min at 4 °C, the supernatant S-12 fraction was collected. The microsomal fraction was collected by centrifugation of the S-12 fraction at 100,000 ×*g* for 60 min at 4 °C. Protein enrichment was ensured by using the Amicon Ultra-0.5 Centrifugal Filter 10 K Devices from Merck Millipore (Darmstadt, Germany). Quantification of total protein was done with the Pierce 660 nm Protein colorimetric assay (Thermo Scientific, Rockford, USA) using protein standards made of bovine serum albumin (BSA). The absorbance at 660 nm was measured spectrophotometrically using a 96-well plate reader.

After SDS-PAGE (10% SDS-gels) using BioRad MiniProtean Cell, proteins were transferred to a PVDF membrane using the Trans-Blot Turbo RTA Transfer kit (BioRad, California, USA). After protein transfer, the membrane was blocked with 3% BSA in 1 × PBS for 60 min at room temperature at continuous shaking. Primary antibodies used for the detection of cytochrome P450 1A (CYP1A) and β-actin (control) were applied to the membrane and incubated overnight at continuous shaking at 4 °C. After second incubation the membrane was rinsed three times for 5 min with 1 × PBS and the secondary antibody (anti-rabbit conjugated to HRP) diluted 1:1000 in 2% ECL in 1 × PBS was added. The membrane was then incubated for 2 h at continuous shaking. After the third incubation the membrane was rinsed again five times for 5 min with 1 × PBS. The PVDF membrane was then exposed to Amersham ECL Western Blotting Detection Reagent (GE Healthcare) for visualization of immunoreactive proteins, using a ChemiDoc camera (G:BOX, Syngene, Cambridge, United Kingdom). Densitometric data analysis was done using the ImageJ software. Because β-actin was regulated by the treatment and could not be used for normalization, the total protein stock pooled from all samples was used for normalization purpose.

2.6. Metabolite analysis

Global metabolite profiling was conducted as previously described by Olsvik et al. (2015). Briefly, samples prepared using the automated MicroLab STAR® (Hamilton Company, Reno, NV, USA) were divided into 5 fractions: one for analysis by Ultrahigh Performance Liquid Chromatography-Tandem Mass Spectroscopy (UPLC-MS/MS) with positive ion mode electrospray ionization, one for analysis by UPLC-MS/MS with negative ion mode electrospray ionization, one for LC polar platform, one for analysis by Gas Chromatography-Mass Spectroscopy (GC–MS), and one sample was reserved for backup. The LC/MS portion of the platform was based on a Waters ACQUITY ultra-performance liquid chromatography (UPLC) and a Thermo Scientific Q-Exactive high resolution/accurate mass spectrometer interfaced with a heated electrospray ionization (HESI-II) source and Orbitrap mass analyzer operated at 35,000 mass resolution. The GC–MS portion of the platform was based on a Thermo-Finnigan Trace DSQ fast-scanning single-quadrupole mass spectrometer using electron impact ionization (EI) and operated at unit mass resolving power.

2.7. Statistics

One-way or two-way ANOVA with Holm-Sidak's posttest was used for comparison between the treatment groups. Brown-Forsythe and Bartlett's tests were used for evaluation of homogeneity of variances, and the values were log-transformed before ANOVA if deemed necessary. Spearman's rank correlation analysis was used to search for possible co-regulation among the parameters. The GraphPad Prism 8.0 (GraphPad Software, Inc., San Diego, CA, USA) was used for statistical analyses of the data. Following normalization to total protein (Bradford assay) and log transformation, and imputation of missing values, if any, with the minimum observed value for each compound, ANOVA contrasts were used to identify metabolites that differed significantly between experimental groups. Welch's two-sample *t*-tests were used to identify metabolites that differed significantly between experimental groups ($p < .05$). Statistical analyses of the log-transformed data were performed with the program "R" (The Comprehensive R Archive Network). Functional pathway analyses were generated through the use of Qiagen's Ingenuity® Pathway Analysis (IPA®, Qiagen Redwood City, www.qiagen.com/ingenuity). IPA Upstream Regulator analytic was used to identify the cascade of upstream transcriptional regulators that can explain the observed expression changes in the datasets.

3. Results

3.1. No effect on cytotoxicity

After extraction, the cell viability was 96 ± 2% ($n = 6$, mean ± st.dev.) as determined with the Trypan Blue exclusion method. After 48 h of exposure, no significant effect of CPF treatment was observed on cytotoxicity measured with the MTT assay or with the xCELLigence system (Fig. S1). Supplementation of ARA or EPA, alone or in combination with CPF, neither had any significant effect on cytotoxicity compared to the control.

3.2. Modified lipid composition of hepatocytes supplemented with PUFAs

Supplementation of ARA and EPA in the exposure medium had a distinct effect on the PUFA profiles of the Atlantic salmon primary cells. Table 1 shows the concentrations of *n*-3 and *n*-6 PUFAs in the hepatocytes. Fig. 1 shows principal component analysis (PCA) plots of the sum of *n*-3 (Fig. 1A) and *n*-6 (Fig. 1B) PUFAs in the cells after the different treatments. Treatment with ARA for 48 h significantly increased the concentration of *n*-6 PUFAs ARA (20:4, 8.5-fold), adrenate (docosatetraenoic acid), (22:4, 38.2-fold), and docosapentaenoate (22:5, 7.5-fold), and decreased linoleate (18:2, −1.9-fold). Treatment with ARA also increased the level of dihomo-linolenate (20:3, *n*-3 or *n*-6, 1.6-fold) and decreased the level of *n*-3 docosahexaenoate (DHA; 22:6, −1.6-fold). Similarly, treatment with EPA for 48 h increased the levels of *n*-3 PUFAs EPA (20:5, 4.3-fold), docosapentaenoate (DPA; 22:5, 6.7-fold) and stearidonate (18:4, 1.5-fold). Treatment with EPA also significantly decreased the levels of linolenate (LA, alpha or gamma, 18:3 *n*-3 or *n*-6, −2.2-fold) and docosapentaenoate (DPA; 22:5, −2.1-fold). Supplementation of ARA or EPA in the culture medium for 48 h significantly changed the fatty acid composition of the Atlantic salmon hepatocytes as intended.

3.3. Steatosis assay and evaluation of lipid droplet formation

Compared to the control, no significant effect of the treatments was seen on steatosis as quantified with the Cayman Steatosis Colorimetric Assay (Fig. 2A). Posthoc tests showed a significant difference in lipid accumulation between cells exposed to CPF and those co-treated with CPF and both PUFAs (one-way ANOVA, $p = .0372$). The degree of lipid accumulation in Atlantic salmon liver cells correlated significantly with the transcriptional levels of peroxisome proliferator activated receptor alpha (*ppara)* (Fig. 2C) and the concentration of DHA and LA (Spearman's rank correlation, *ppara*: $p = .002$, $r = 0.34$; *n*-3 DHA: $p = .03$, $r = 0.20$ and *n*-6 LA: $p = .031$, $r = 0.22$).

Three methodological approaches were used to examine how CPF, ARA and EPA affect lipid droplet accumulation and morphology. First by examining the visible impact on overall histology, secondly by the quantification of total number and area of lipid droplets and thirdly by a quantitative assessment of lipid droplet size. Fig. 3 shows representative images of lipid droplets in the hepatocytes after treatment. From the images, it can clearly be seen that ARA and EPA supplementation, alone or in combination with CPF, strongly impacts lipid droplet formation (Fig. 3C–G). Exposure to CPF alone (Fig. 3B) also appears to slightly increase lipid formation in the hepatocytes. In addition, there were noticeably larger sized lipid droplets in hepatocytes exposed individually to ARA and EPA, and the different combinations

Table 1
Profile of polyunsaturated fatty acids (PUFAs) in Atlantic salmon hepatocytes after 48 h exposure to chlorpyrifos (CPF) and supplementation with 200 μM arachidonic acid (ARA) or eicosapentaenoic acid (EPA) (values based on raw area counts normalized by Bradford protein).

Polyunsaturated fatty acid	Control	CPF	ARA	CPF + ARA	EPA	CPF + EPA	CPF + ARA + EPA
n-3 PUFAs							
Stearidonate (18:4*n*-3)	1.574 ± 0.495	0.727 ± 0.198**	1.671 ± 0.532	0.814 ± 0.142**	2.387 ± 0.590	0.876 ± 0.233*	0.805 ± 0.257**
Eicosapentaenoate (EPA; 20:5*n*-3)	0.817 ± 0.145	0.462 ± 0.114***	0.876 ± 0.222	0.443 ± 0.055***	3.504 ± 1.145****	2.222 ± 0.545****	2.295 ± 0.365****
Docosapentaenoate (DPA; 22:5*n*-3)	0.932 ± 0.278	0.389 ± 0.096***	1.065 ± 0.462	0.284 ± 0.061****	6.199 ± 2.418****	2.712 ± 1.010****	1.496 ± 0.516
Docosahexaenoate (DHA; 22:6*n*-3)	2.794 ± 0.630	0.969 ± 0.251****	1.716 ± 0.495**	0.364 ± 0.076****	2.791 ± 0.761	0.579 ± 0.166****	0.321 ± 0.054****
Docosatrienoate (22:3*n*-3)	1.622 ± 0.780	0.885 ± 0.339	3.486 ± 2.709	1.430 ± 0.943	1.349 ± 0.583	0.426 ± 0.195***	0.414 ± 0.173***
n-3 or *n*-6 PUFAs							
Linolenate (alpha or gamma; 18:3*n*-3 or *n*-6)	1.778 ± 0.479	1.009 ± 0.211**	1.835 ± 0.484	1.046 ± 0.096**	0.824 ± 0.163****	0.453 ± 0.101****	0.485 ± 0.133****
Dihomo-linolenate (20:3*n*-3 or *n*-6)	1.336 ± 0.241	0.789 ± 0.126**	2.180 ± 0.842**	1.209 ± 0.212	1.131 ± 0.172	0.503 ± 0.068****	0.690 ± 0.150****
n-6 PUFAs							
Arachidonate (ARA; 20:4*n*-6)	0.746 ± 0.220	0.397 ± 0.099***	6.336 ± 1.562****	5.165 ± 0.906****	0.826 ± 0.224	0.386 ± 0.083***	4.341 ± 0.490****
Adrenate (22:4*n*-6)	0.795 ± 0.337	0.289 ± 0.188***	30.33 ± 9.125****	16.41 ± 2.844****	0.981 ± 0.406	0.473 ± 0.279	7.780 ± 2.141****
Linoleate (18:2*n*-6)	1.880 ± 0.411	1.397 ± 0.316	0.973 ± 0.350***	0.637 ± 0.123****	1.472 ± 0.313	0.946 ± 0.171***	0.519 ± 0.106****
Docosapentaenoate (DPA; 22:5*n*-6)	0.592 ± 0.247	0.430 ± 0.102	4.457 ± 2.612****	1.422 ± 0.561***	0[a]	0[a]	0[a]
Docosadienoate (22:2*n*-6)	2.142 ± 1.327	1.422 ± 0.647	1.646 ± 0.669	0.670 ± 0.087***	1.481 ± 0.432	0.504 ± 0.099****	0.422 ± 0.089****
Dihomo-linoleate (20:2*n*-6)	2.075 ± 0.784	1.200 ± 0.358*	1.474 ± 0.599	0.763 ± 0.096****	1.339 ± 0.218	0.626 ± 0.122****	0.505 ± 0.151****

Stars indicate significant differences as compared to the control (one-way ANOVA with Holm-Sidak's multiple comparisons test, using log-transformed data, $^{*}p < .05$, $^{**}p < .01$, $^{***}p < .001$, $^{****}p < .0001$). Data are expressed as means ± st.dev. ($n = 6$).
[a] Below detection limit, missing values are imputed with the minimum.

of CPF, ARA and EPA, compared to the control group. Fig. 4A shows the total number of lipid droplets in equally sized and squared areas of the images. Compared to the control, all treatment groups that received PUFAs had significantly higher number of lipid droplets. Exposure to CPF alone did not significantly increase the number of lipid droplets in the cells. Quantitative examination of the total area of lipid droplets yielded the same pattern, with larger areas covered by lipid droplets in cells treated with PUFAs (Fig. 4B). Size distribution of lipid droplets are shown in Table 2. For small-sized lipid droplets ($< 0.5\,\mu m^2$), the treatment reduced the number of lipid droplets in the CPF + ARA and CPF + EPA groups compared to the control (one-way ANOVA, $p < .01$). For the medium-sized range ($5–15\,\mu m^2$), treatment with ARA, CPF + ARA and CPF + EPA increased the number of lipid droplets ($p < .05$). No significant differences were observed for large-sized ($15–30\,\mu m^2$) and very large-sized ($> 30\,\mu m^2$) lipid droplets.

3.4. *Ppara and fabp3 transcription affected by chlorpyrifos*

Of 9 examined target genes, only 2 showed a significant induction after CPF treatment. For *ppara* (Fig. 2C) and fatty acid binding protein 3 (*fabp3*) (Fig. 2D) there were significant effects of CPF treatment (2-way ANOVA, *ppara*: $p = .0029$, *fabp3*: $p = .0036$). No significant interaction effect of co-treatment with ARA or EPA was seen on the transcription of these genes. Although not significant, for *ppara* it appeared that co-treatment with EPA but not ARA weakened the CPF-induced effect. For *cyp1a1* transcription (Fig. 2E), there was a significant effect of ARA and EPA treatment (reduced transcriptional levels) (2-way ANOVA, ARA: $p = .0207$, EPA: $p = .0159$), but no interaction effect with CPF and the PUFAs, or effect of CPF alone. According to the 2-way ANOVA result, a significant effect of ARA treatment was also seen on *daf36* (2-way ANOVA, $p = .0075$), but again with no interaction effect with CPF (Fig. S2F). No significant effects were seen for *cyp3a*, *vtg1*, *cpt1a*, *acox1* and *rara* (Fig. S2).

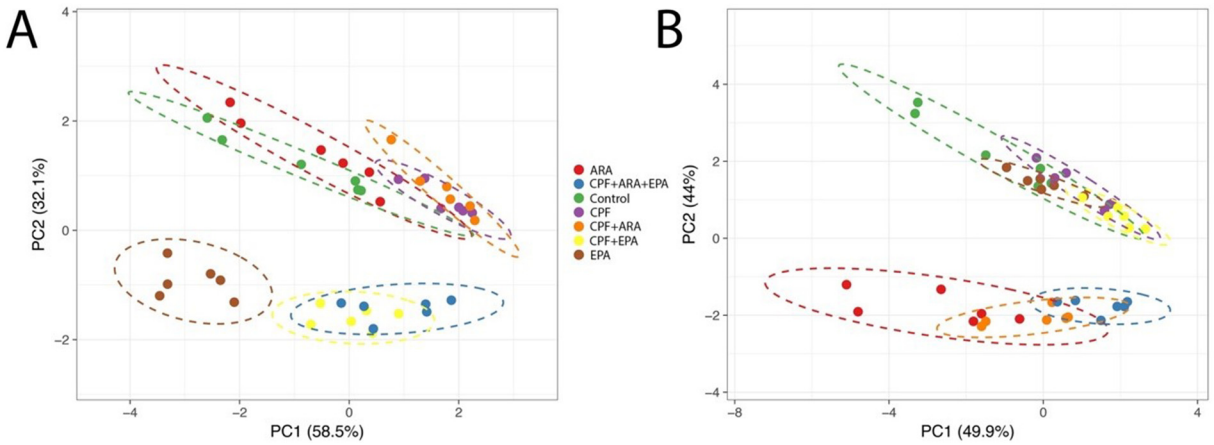

Fig. 1. Principal component analysis (PCA) showing treatment effects on (A) sum of *n*-3 fatty acids (Σ EPA, DHA, *n*-3 DPA, SDA and docosatrienoate (22:3) and (B) sum of *n*-6 fatty acids (Σ ARA, *n*-6 DPA, adrenate (22:4), dihomo-linoleate (20:2), docosadienoate (22:2), linoleate (18:2)).

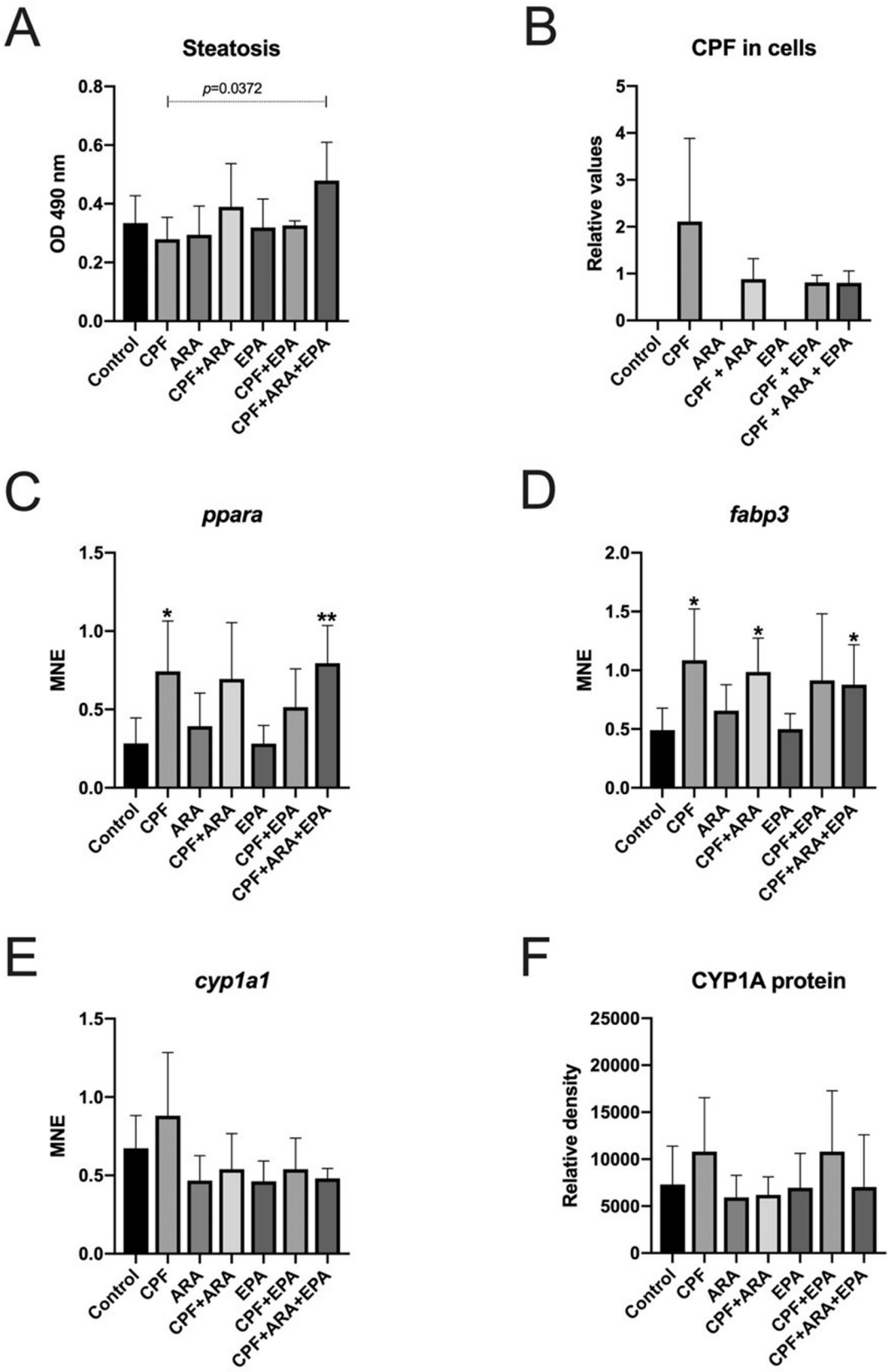

Fig. 2. (A) Steatosis in Atlantic salmon hepatocytes exposed to chlorpyrifos (CPF) alone or in combination with arachidonic acid (ARA) and eicosapentaenoic acid (EPA) determined with a colorimetric assay. (B) CPF levels in exposed cells, (C) *ppara* gene expression, (D) *fabp3* gene expression, (E) *cyp1a1* gene expression and (F) CYP1A protein level. Significance levels (two-way ANOVA, Holm-Sidak's post-test) are shown in the figures. $^{*}p < .05$, $^{**}p < .01$. For the comparison between the control and CPF + ARA + EPA group, significance is shown based on the t-test. Values are mean ± st.dev. ($n = 6$).

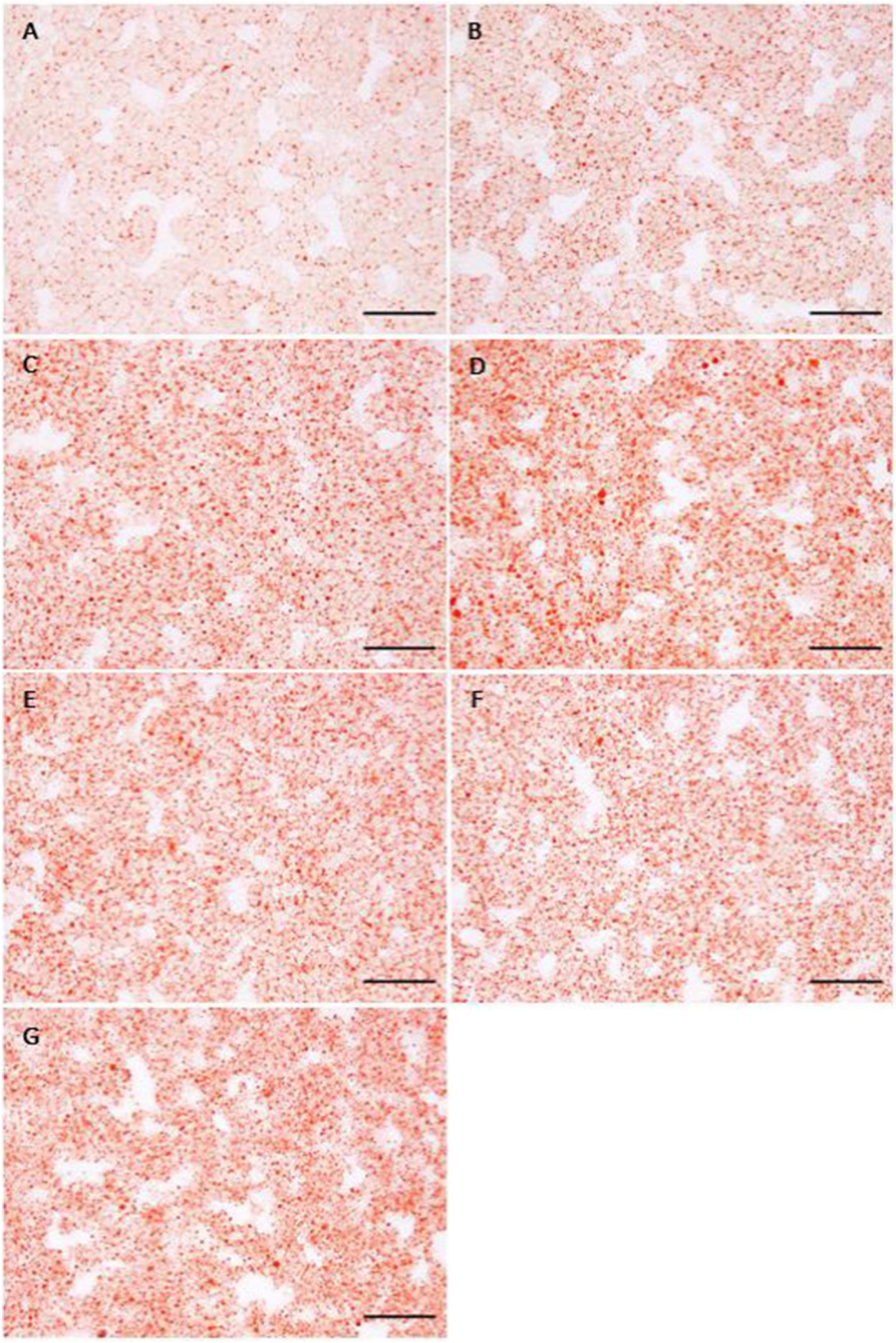

Fig. 3. Representative microscopy images of primary hepatocytes from Atlantic salmon exposed to chlorpyrifos (CPF), arachidonic acid (ARA) and eicosapentaenoic acid (EPA) individually or in combination and stained with Oil Red O. (A) Control, (B) CPF (100 μM), (C) ARA (200 μM), (D) CPF (100 μM) + ARA (200 μM), (E) EPA (200 μM), (F) CPF (100 μM) + EPA (200 μM), and (G) CPF (100 μM) + ARA (200 μM) + EPA (200 μM). The presented images are representative for the morphological changes seen in different exposure groups ($n = 6$). The magnification was set to 20×, scale bar = 100 μm, picture resolution 4.1681 pixel/μm. (For interpretation of the references to colour in this figure legend, the reader is referred to the web version of this article.)

3.5. No effect on CYP1A protein level

No significant effects were seen for CYP1A (Fig. 2F) protein content in the cells after the different treatments.

3.6. Impact of PUFAs on metabolites

A total of 330 metabolites with known ID were detected in the Atlantic salmon hepatocytes. Table 3 shows a summary of the numbers of metabolites and biochemicals that achieved statistical significance ($p \leq .05$). Overlapping metabolites are shown in Fig. 5A, B. Supplementary File 2 shows all individual metabolites that were significantly affected by the various treatments. Principal component analysis revealed a certain degree of heterogeneity within the controls and in the group exposed to CPF (data not shown), potentially suggesting differences in basal metabolism between individual primary-derived cell samples or CPF induced differences in cellular metabolism. Hierarchical clustering still showed a relatively clear separation between the groups that received CPF or not (Fig. 5C). Combinatorial treatment with CPF resulted in a shift compared to single treatment alone and may reflect an additive or synergistic impact on global metabolism.

IPA Upstream Regulator analytic was used to identify the cascade of upstream transcriptional regulators that can explain the observed changes in the datasets. A combined list of significant genes and metabolites were used as input for the IPA analyses. Predicted upstream regulators are shown in Supplementary File 3.

3.6.1. PUFA supplementation reduces chlorpyrifos accumulation

The metabolic profiling documented significant accumulation of CPF in hepatocytes after 48 h of treatment (Fig. 2B). Cells that were co-

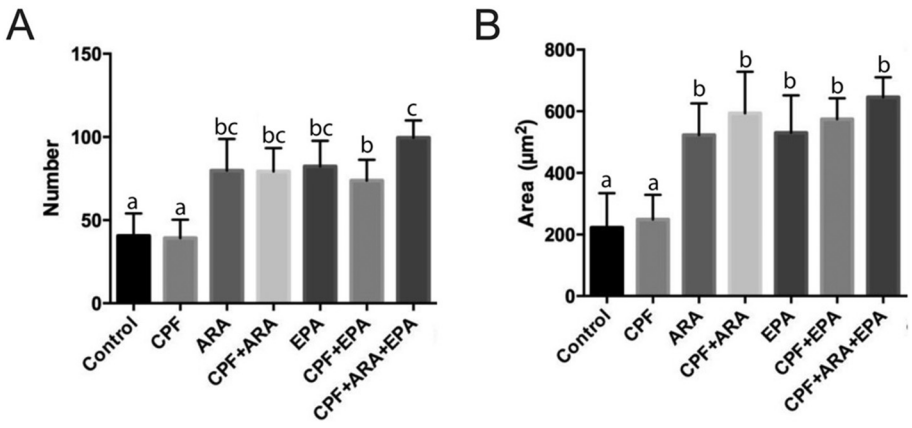

Fig. 4. Total number (A) and total area (B) of lipid droplets in Atlantic salmon hepatocytes exposed to chlorpyrifos (CPF), arachidonic acid (ARA), eicosapentaenoic acid (EPA), and combinations of CPF, ARA and EPA. Primary hepatocyte cells were stained with Oil Red O and evaluated under light microscopy. Different letters indicate statistical differences in mean values between the different treatment groups (one-way ANOVA, $p < .05$). Values are mean ± st.dev. ($n = 6$). (For interpretation of the references to colour in this figure legend, the reader is referred to the web version of this article.)

Table 2
Size distributions of lipid droplets in Atlantic salmon hepatocytes. Values are given as mean ± st.dev. ($n = 6$).

Treatment	Small	Medium	Large	Very large
	< 5 µm²	5–15 µm²	15–30 µm²	> 30 µm²
Control	71.6 ± 8.7	27.0 ± 15.2	2.5 ± 2.8	0.7 ± 1.8
CPF	48.6 ± 18.9	45.5 ± 10.6	5.4 ± 9.0	0.5 ± 1.1
ARA	44.4 ± 18.1	51.1 ± 17.1*	3.8 ± 2.3	0.7 ± 1.4
CPF + ARA	37.3 ± 16.3**	54.6 ± 13.5*	7.3 ± 4.1	0.8 ± 1.1
EPA	44.7 ± 15.7	50.7 ± 12.1	4.4 ± 4.0	0.2 ± 0.5
CPF + EPA	38.4 ± 13.7**	52.9 ± 13.0*	7.5 ± 2.7	1.2 ± 1.4
CPF + ARA + EPA	47.6 ± 9.0	47.2 ± 7.0	4.5 ± 2.6	0.7 ± 0.9

Asterisks indicate statistical differences in mean values between exposures within each group of size (one-way ANOVA, $p < .05$). *$p < .05$, **$p < .01$. Chlorpyrifos (CPF), arachidonic acid (ARA), eicosapentaenoic acid (EPA).

treated with ARA, EPA or both PUFAs contained significantly lower levels of CPF than cells that only received CPF (one-way ANOVA, $p = .0337$ for all comparisons, using imputation values for cells with no detectable levels of CPF). Accumulation of CPF in the cells correlated with the transcriptional levels of *ppara* and *fabp3*, and with the concentration of almost all *n*-3 and *n*-6 PUFAs detected in the cells, including ARA (20:4), EPA (20:5), and DHA (22:6) (Spearman's rank correlation analysis, $p < .05$).

3.6.2. Chlorpyrifos exposure reduced the levels of PUFAs in cells

In the presence of CPF alone, significantly diminished levels of multiple *n*-3 and *n*-6 PUFAs (in total 9 were diminished) including EPA, DHA, LA, and ARA were observed (Table 1). As expected, co-treatment with EPA diminished the impact CPF had on *n*-3 EPA and DPA (Fig. 6A). Co-treatment with ARA, on the other hand, enhanced the impact CPF had on DHA, a response not rescued by adding EPA. Similarly, supplementation with ARA counteracted the impact CPF had on *n*-6 ARA and adrenate, but not *n*-3 PUFAs. For the PUFAs, interaction effects between CPF and ARA were observed for *n*-6 adrenate and DPA, while interaction effect between CPF and EPA was only observed for *n*-3 DPA (2-way ANOVA, $p < .05$). These findings suggest that supplementation of ARA and EPA had low impact on the CPF-induced effects on PUFAs other than ARA and EPA in the cells.

3.6.3. Monoacylglycerols (MAGs) strongly affected by chlorpyrifos

One of the most distinct effect of CPF was the strong degree of accumulation of MAGs in exposed cells. Compared to the control, 15 species of MAG were increased in cells exposed to CFP (Table 4). EPA supplementation resulted in a similar pattern, with 13 MAG species showing significantly higher concentrations compared to the control. In contrast, only 3 MAGs were elevated in cells supplemented with ARA (1-arachidonylglycerol (20:4), 2-arachidonoylglycerol (20:4) and 1-dihomo-linolenylglycerol (20:3)). Co-treatment with either ARA or EPA does not seem to have any significant impact on the CPF-induced effect on MAGs in the cells. CPF treatment also reduced the levels of glycerol in the cells (Fig. 6B).

Several long-chain fatty acids, palmitoleate (16:1n7), oleate (18:1n9), myristoleate (14:1n5), 10-heptadecenoate (17:1n7), and cis-vaccenate (18:1n7), were diminished in CPF-treated hepatocytes compared to controls (Supplementary File 2). As for the MAGs, this trend was observed in each treatment condition independent of PUFA supplementation or combinatorial treatment.

3.6.4. Reduced energy metabolism

An impact of CPF on energy metabolism was indicated with reduced levels of the glycogen metabolites maltopentaose, maltotetraose, maltotriose, and maltose in exposed cells compared to the controls (Fig. 6C). This trend was partially rescued in CPF cultures by combinatorial treatment with ARA or EPA, but not together. Reduced levels of glucose in the presence of CPF were accompanied by diminished fructose 1,6-bisphosphate, dihydroxyacetone phosphate (DHAP), and lactate, indicating a decline in glycolytic metabolism and energy generation. Similar to glucose, ARA and EPA supplementation alone with CPF, but not in combination (CPF + ARA + EPA) was able to partially rescue lactate and pyruvate, indicating a restoration of glycolysis and energy metabolism. Increased levels of the TCA cycle intermediates alpha-ketoglutarate, succinate, and fumarate (the latter two with $p < .10$) in cells treated with CPF further indicate an impact on overall energy metabolism (Fig. 6C). ARA and EPA supplementation were able to restore these energy metabolites to control levels in the presence of CPF, indicating that supplementation of *n*-3 and *n*-6 PUFA can partially rescue this deficit.

3.6.5. Moderate oxidative stress

A certain degree of oxidative stress was indicated by low levels of reduced glutathione (GSH) accompanied by modest accumulation of oxidized glutathione (GSSG), in addition to significantly reduced levels of cysteine, in CPF-treated cells. Furthermore, significantly diminished levels of hypotaurine, taurine, and cysteine-glutathione disulfide also suggested limited cysteine availability or preferential utilization for glutathione synthesis (Fig. 6D). ARA and EPA supplementation were not able to counteract this response in the cells.

4. Discussion

In salmonids, it is well known that the cellular fatty acid profile of tissues such as the liver is highly influenced by both dietary and environmental factors (Olsvik et al., 2011; Cornet et al., 2018). Supplementation of free fatty acids in the medium will also change the fatty acid profile of salmonid cells in culture (Ferain et al., 2016). In this study, the fatty acid profile of the cells supplemented with ARA and

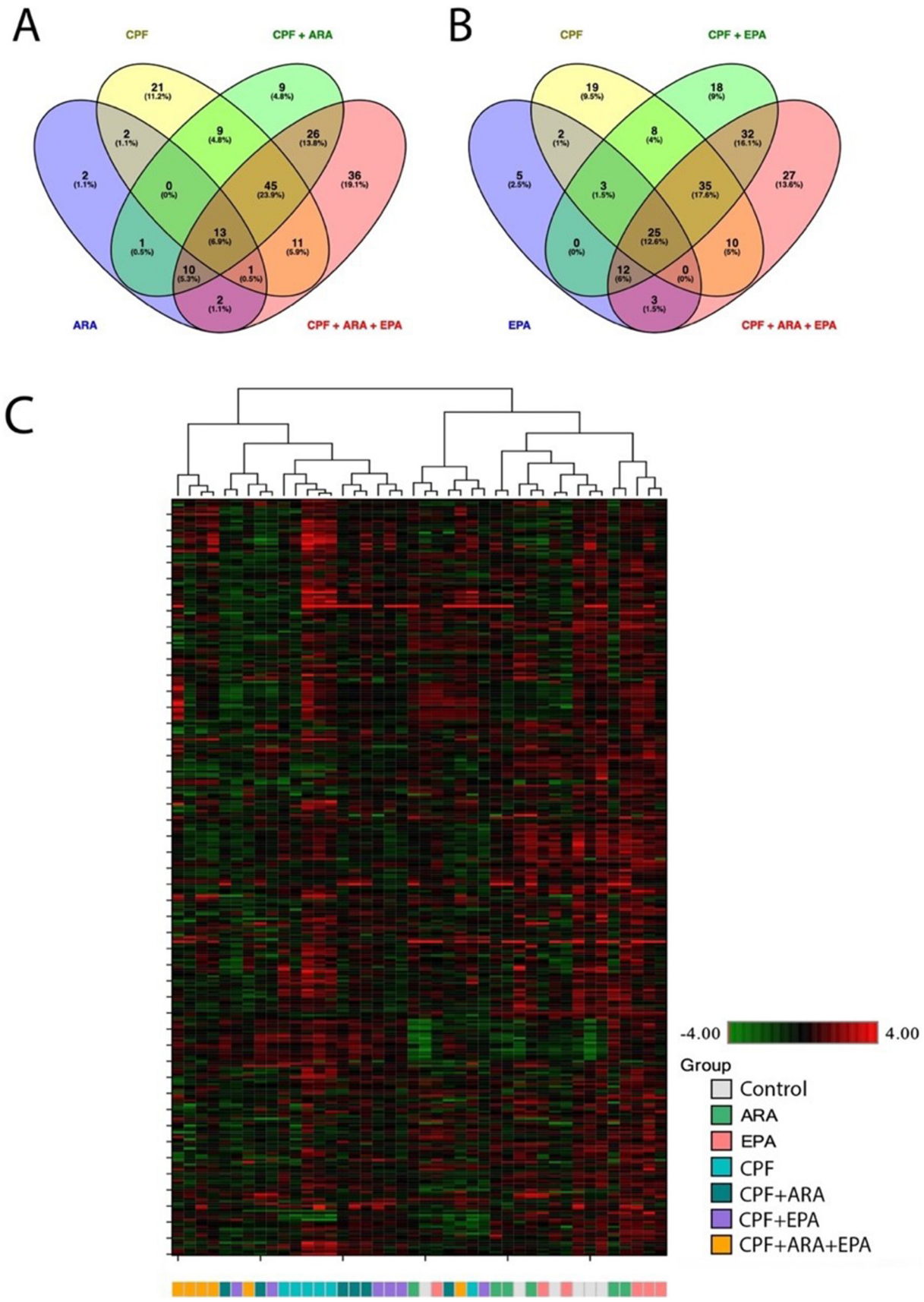

Fig. 5. Venn diagram showing the number of metabolites affected by co-treatment of chlorpyrifos (CPF) and (A) arachidonic acid (ARA) and (B) eicosapentaenoic acid (EPA). (C) Hierarchical clustering of metabolites.

Table 3
Number of significantly affected biochemicals in Atlantic salmon hepatocytes exposed to chlorpyrifos (CPF) and co-treated with combinations of arachidonic acid (ARA) and eicosapentaenoic acid (EPA).

Treatment	Significantly altered biochemicals	Directional response
	$p < .05$	(↑ I ↓)
CPF	102	34 I 68
ARA	31	13 I 18
CPF + ARA	113	25 I 88
EPA	50	19 I 31
CPF + EPA	133	21 I 112
CPF + ARA + EPA	144	34 I 110

EPA clearly reflected this, with elevated levels of *n*-3 PUFAs in cells given EPA and *n*-6 PUFAs in cells given ARA. Lipid droplet staining confirmed that PUFA supplementation had a profound effect on the cells. Both the number and size of lipid droplet increased by adding ARA and EPA. Primary culture of Atlantic salmon hepatocytes therefore seems to be well suited to study the impact of altered phospholipid composition on the toxicity of contaminants.

In contrast to PUFA supplementation and combinations between CPF and PUFAs, exposure to CPF alone did not significantly increase the number of lipid droplets in the cells. For medium and large-sized lipid droplets, however, CPF treatment doubled the number, but the increase was not significant. For small-sized lipid droplets the insecticide reduced the number, but again the difference was not significant. This finding was supported by the metabolite profiling. According to IPA Core Analysis, "Accumulation of TAG" was reduced in all treatment groups that received CPF, whereas ARA and EPA supplementation had no impact on this function. In terms of steatosis with TAG accumulation in lipid droplets, this study does not document any effect of CPF. The lack of significant increase in the number of lipid droplets in this study can rely on the dose, as exposure to high concentrations of OPs reportedly can induce accumulation of TAG and emergence of large lipid droplets in fish liver (Du et al., 2016).

This study clearly demonstrates that exposure to CPF leads to disruptive lipid metabolism in Atlantic salmon hepatocytes. Most prominently, CPF exposure reduced the levels of 10 different *n*-3 and *n*-6 PUFAs and 5 long-chain fatty acids, and lead to accumulation of 15 MAGs in liver cells. This result is broadly in line with our previous exposure studies with OPs and Atlantic salmon hepatocytes (Olsvik et al., 2015, 2017). Supplementation with EPA in the exposure medium did not prevent the CPF-induced impacts on most PUFAs and long-chain fatty acids, except for increasing the levels of EPA itself and *n*-3 DPA. Co-treatment with EPA strengthened the effect on long-chain fatty acids. While EPA alone only lowered the levels of two long-chain fatty acids, CPF and EPA together resulted in lower levels of 15 long-chain fatty acids in the cells. The same pattern was seen for the MAGs. CPF treatment resulted in elevated levels of 15 MAGs, while EPA supplementation increased the levels of 13 MAGs. CPF and EPA co-treatment increased the levels of 15 MAGs. In comparison, ARA supplementation had much less effect on these lipid species. Treatment with ARA had no effect on the levels of long-chain fatty acids. Apart from increasing the level of ARA itself 8.5-fold, and subsequently increasing the levels of 4 other *n*-6 PUFAs (LA, adrenate, *n*-6 DPA and dihomo-linolenate), ARA supplementation lowered the level of DHA. The most distinct effect of co-treatment of both PUFAs and CPF was seen for *n*-6 DPA. The levels of *n*-6 DPA were increased in cells given ARA (7.5-fold) and CPF + ARA (2.4-fold), but not in cells given CPF + ARA + EPA (−2.0-fold). ARA supplementation also had less impact on MAG accumulation than CPF and EPA. Only 3 MAGs were elevated in cells treated with ARA. Combined treatment with EPA (CPF + ARA + EPA) did not alter this pattern. Overall, culture supplementation with ARA and/or EPA only modestly affects the impact CPF has on PUFAs in the cells.

Accumulation of MAGs in CPF-exposed cells suggests a potential change in complex lipid metabolism that may correlate with reduced long-chain fatty acid availability. Less TAG will be generated with reduced availability of long-chain fatty acids. Alternatively, increased accumulation of MAGs results from inhibited monoacylglycerol lipase (MGLL) activity. Indeed, IPA Core Analysis predicted monoacylglycerol lipase (MGLL) as one of the most significant upstream regulators explaining the response to CPF treatment. The activation score of MGLL was predicted decreased to a similar degree in cells exposed to CPF, CPF + ARA and CPF + EPA. When co-treated with a combination of both PUFAs, this response disappeared. MGLL is responsible for the complete hydrolysis of MAGs into glycerol and free fatty acids (Zechner et al., 2012). Glycerol and glycerol 3-phosphate were both strongly diminished in cell given all combinations containing CPF, either as a result of decreased availability of free fatty acids or decreased lipolysis (or both). Supplementation with PUFAs had no impact on this response, although EPA alone significantly increased glycerol compared to the control. Only 2 metabolites directly linked to phospholipid metabolism, glycerophosphorylcholine (GPC) and glycerophosphoinositol, were significantly affected by CPF exposure. PUFA supplementation could not restore the diminished levels of these metabolites in salmon hepatocytes. In addition, 3 lysolipids, 1-palmitoyl-GPC (16:0), 1-palmitoleoyl-GPC (16:1) and 1-oleoyl-GPC (18:1), were significantly elevated in cells exposed to CPF. These responses were countered by the PUFAs, most prominently by EPA.

In addition to increased transcription of *ppara* and *fabp3*, there were several indications of altered β-oxidation of fatty acids in the CPF-exposed cells. Intracellular concentrations of fatty acids and their derivatives are strictly regulated (Reddy and Hashimoto, 2001). Activation of PPARA, a transcriptional regulator of genes involved in peroxisomal and mitochondrial β-oxidation, as well as fatty acid transport, has been shown to improve steatosis and inflammation in rodent models (Staels et al., 2013). Elevated levels of acetylcarnitine, which contributes to the movement of acetyl CoA in the mitochondria during lipid oxidation (Reddy and Hashimoto, 2001), may be indicative of a change in free carnitine levels as acetylcarnitine is often broken down by esterases to carnitine in order to support the transport of fatty acids. Furthermore, low levels of carnitine and deoxycarnitine may suggest a limited capacity to facilitate mitochondrial β-oxidation as evidenced by low levels of the ketone body 3-hydroxybutyrate (generated in the presence of excess acetyl-CoA and historically a marker of fatty acid oxidation). These perturbation in lipid oxidation were consistent with our previous study (Olsvik et al., 2015) and were modestly rescued by EPA supplementation alone or in combination with ARA.

In line with our previous study (Olsvik et al., 2015), CPF showed a distinct effect on many metabolites associated with energy metabolism, *i.e.* glycolysis and TCA cycle intermediates. Reduced levels of glycogen metabolites may reflect decreased glycogen stores or a decline in glycogen degradation that consequently limited glucose levels in these cells. Furthermore, accumulation of pyruvate in exposed cells point to a defect in lactate dehydrogenase (LDH) function. The effects on TCA metabolites may be indicative of mitochondrial dysfunction and potential inhibition of enzymes, as has been reported after exposure to OPs in fish and human cells (Almeida et al., 2010; Yamada et al., 2017). ARA and EPA supplementation alone, but not in combination, was able to partially rescue glycogen degradation, as well as lactate and pyruvate levels. Taken together, these findings suggest that CPF may limit the energetic capacity of the liver cells, a mechanism partly restored by *n*-3 and *n*-6 PUFA supplementation.

Secondary effects of CPF in fish often include oxidative stress. Numerous studies have reported that oxidative stress is one of the main effects of CPF in fish after waterborne exposure (Oruc, 2010; Xing et al., 2012). In line with the current study, exposure of salmon hepatocytes to OPs also typically results in diminished levels of reduced GSH and altered levels of cysteine, the rate-limiting metabolite for glutathione biogenesis (Olsvik et al., 2015). Collectively, these observations

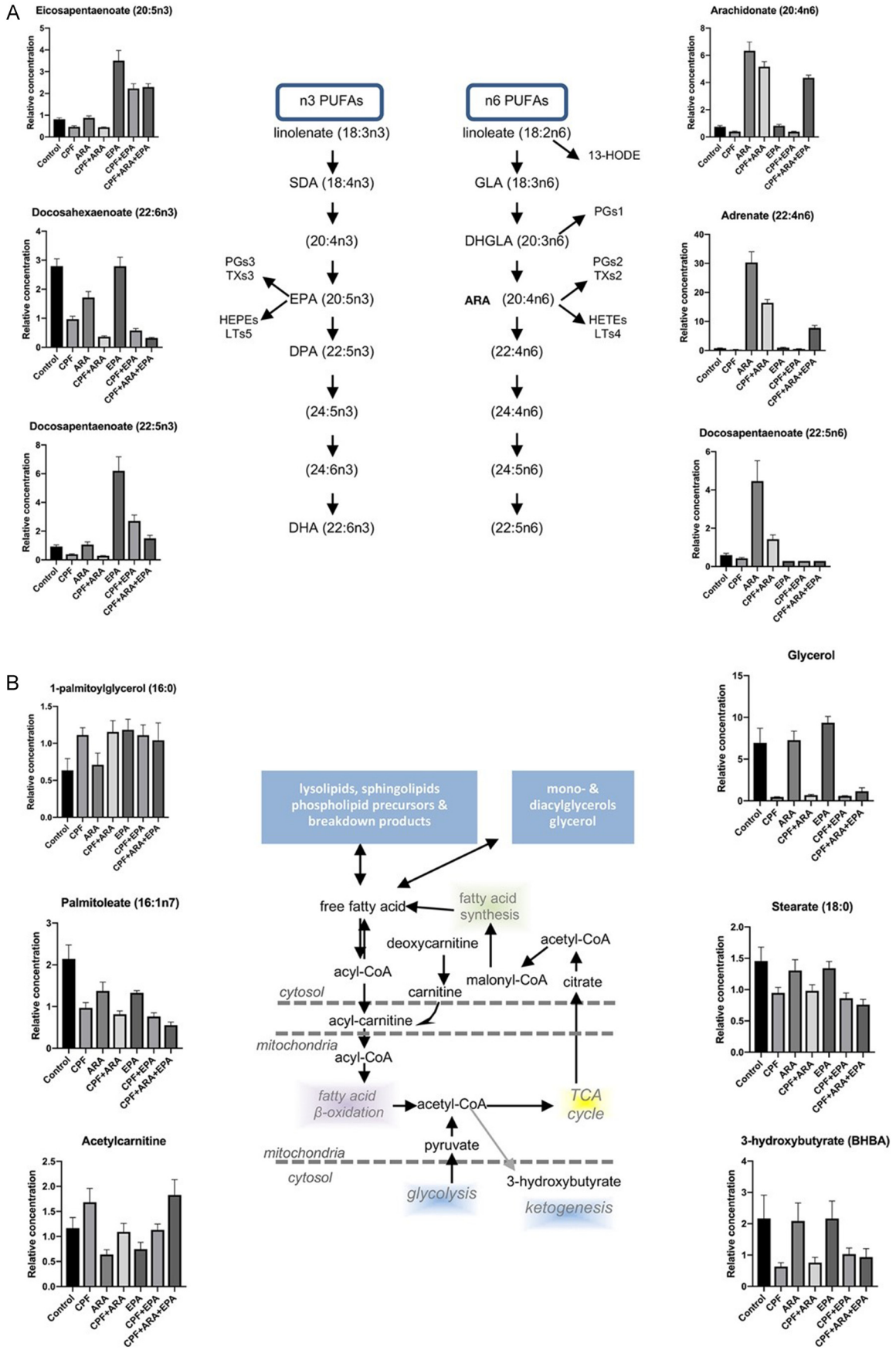

Fig. 6. Pathways affected by chlorpyrifos (CPF), arachidonic acid (ARA), eicosapentaenoic acid (EPA), and combinations of these in Atlantic salmon hepatocytes. (A) *n*-3 and *n*-6 PUFAs, (B) long-chain fatty acids and monoacylglycerol, transport of fatty acids (C) glycolytic metabolism and TCA intermediates and (D) cysteine and glutathione biogenesis. Graphs shows mean ± SEM ($n = 6$).

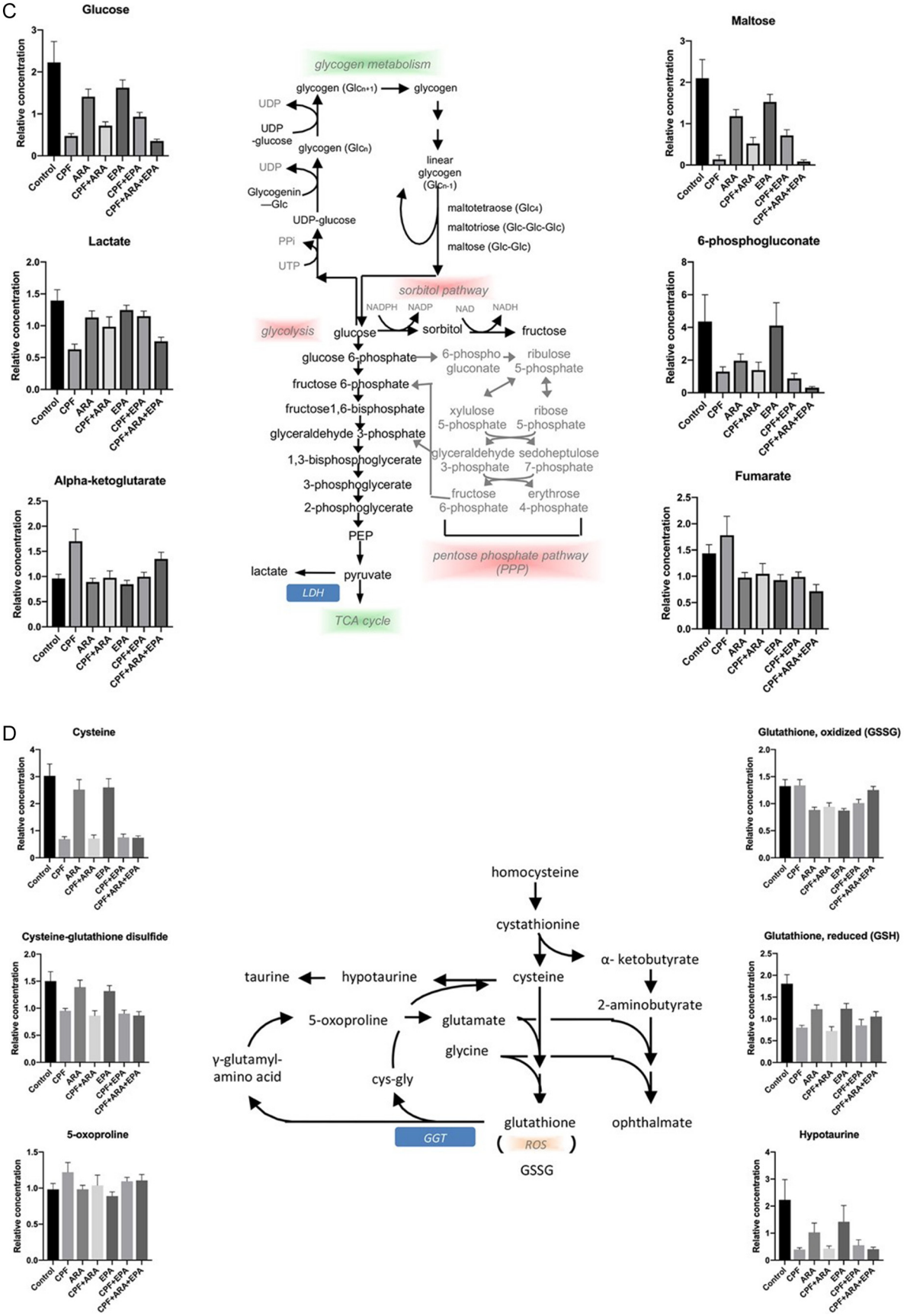

Fig. 6. (*continued*)

Table 4
Monoacylglycerol species affected by chlorpyrifos (CPF), arachidonic acid (ARA) and eicosapentaenoic acid (EPA), and their combinations, in Atlantic salmon hepatocytes. The table shows fold-change ratios (comparisons to the control group). Red (upregulated) $p < .05$. Pink $p < .10/ > .05$.

Monoacylglycerol species	CPF	ARA	CPF+ARA	EPA	CPF+EPA	CPF+ARA+EPA
1-myristoylglycerol (14:0)	2.41	2.69	3.03	2.46	2.58	2.49
2-myristoylglycerol (14:0)	4.60	2.36	3.6	2.17	2.55	1.78
1-pentadecanoylglycerol (15:0)	1.20	1.22	1.59	1.69	1.33	1.19
1-palmitoylglycerol (16:0)	2.36	2.05	2.12	2.19	1.89	1.92
2-palmitoylglycerol (16:0)	3.39	1.95	2.93	2.18	2.85	2.06
2-stearoylglycerol (18:0)	1.83	1.49	1.45	2.52	1.15	1.94
1-oleoylglycerol (18:1)	2.05	1.49	1.93	1.82	1.83	1.43
2-oleoylglycerol (18:1)	3.86	1.22	2.76	1.47	2.48	1.49
1-linoleoylglycerol (18:2)	3.59	2.65	5.24	3.18	3.79	2.97
2-linoleoylglycerol (18:2)	4.71	1.18	3.51	1.57	3.07	1.74
1-linolenoylglycerol (18:3)	4.22	3.3	5.01	2.74	3.90	3.42
1-arachidonylglycerol (20:4)	7.31	15.53	47.91	3.70	6.63	29.38
2-arachidonoylglycerol (20:4)	10.07	7.57	30.26	4.18	7.21	16.62
1-docosahexaenoylglycerol (22:6)	5.88	2.29	6.16	3.45	5.48	4.23
1-dihomo-linolenylglycerol (20:3)	5.63	3.66	7.58	3.10	4.44	4.31
2-docosahexaenoylglcyerol*	12.10	2.32	8.29	2.79	6.82	4.97
1-palmitoleoylglycerol (16:1)*	2.97	2.46	3.74	2.71	3.22	2.40
2-palmitoleoylglycerol (16:1)*	5.55	1.88	4.20	1.77	3.42	2.24

demonstrate that CPF induces oxidative stress in multiple model systems. *n*-3 PUFAs such as EPA has been proposed to have antioxidant properties (Anderson et al., 2014). For example, in fish liver and kidney it has been shown that EPA but not ARA enrichment protects the cells against cadmium and methylmercury, metals that often induce oxidative stress in fish (Nøstbakken et al., 2012; Ferain et al., 2016). However, neither EPA nor ARA supplementation was able to restore the levels of GSH in the cells in this study. A similar response was seen in Atlantic salmon hepatocytes co-treated with CPF and vitamin E (Olsvik et al., 2015). Vitamin E is a potent fat-soluble antioxidant that protects cells from production of ROS when fat undergoes oxidation. Supplementation with 100 µM vitamin E (alpha-tocopherol) did however not restore cysteine metabolism or GSH levels in salmon hepatocytes exposed to CPF (Olsvik et al., 2015).

Of other noticeable CPF-induced metabolic changes restored by PUFA supplementation, pterin and histidine metabolism can specifically be mentioned. The cofactor pterin and the related metabolites biopterin and dihydrobiopterin were significantly reduced in the presence of CPF. Pterins contribute to the generation of folates (also significantly diminished with pesticide treatment) and metabolic processes including hydroxylation of aromatic compounds, the synthesis of nitric oxide, respiratory oxidation, and eye pigmentation (Basu and Burgmayer, 2011). Dihydrobiopterin is a cofactor for the synthesis of tyrosine and the neurotransmitters dopamine and serotonin. Biopterin has been linked to neuron degeneration and dopamine deficiency, while neopterin influences biopterin synthesis and reflects immune activation (Basu and Burgmayer, 2011). Thus, disruptions in pterin metabolism and availability may impact multiple biochemical pathways. The CPF-induced effect on pterin metabolism was rescued by both ARA and EPA supplementation. Furthermore, elevated levels of histidine and the related degradation products trans-urocanate and cis-urocanate were observed in response to CPF treatment. This perturbation did not occur in the presence of ARA or EPA. In Atlantic salmon hepatocytes co-treated with CPF and vitamin E, CPF-induced elevated levels of histidine and trans-urocanate were not restored by the antioxidant (Olsvik et al., 2015). Differences in histidine metabolism can be indicative of protein turnover and matrix remodeling. In summary, PUFA supplementation obviously has the potential to rescue several mechanisms in Atlantic salmon liver cells, not only those solely restricted to lipid metabolism.

Chlorpyrifos is metabolized and detoxified by phase I and II enzymes (Hodgson and Rose, 2008). In Atlantic salmon liver cells, we have previously shown that *cyp1a1* is induced at the transcriptional level at 10 µM but not at 100 µM CPF (Søfteland et al., 2014; Olsvik et al., 2015). After 30 days of dietary exposure to CPF, EROD activity was significantly elevated in Atlantic salmon liver (Sanden et al., 2018), but not in liver of Atlantic cod (*Gadus morhua*) (Olsvik et al., 2019b). In this study, however, no significant effects of CPF exposure were seen on *cyp1a1* or CYP1A protein levels. Cholate and deoxycholate, markers of primary and secondary bile acid metabolism, were significantly elevated in cells exposed to CPF, indicating enhanced detoxification in exposed cells. The levels of these metabolites were lower in cells co-treated with PUFAs, probably reflecting lower uptake of CPF in these cells.

By using hepatocytes from males only, we included *vtg* as a transcriptional marker of potential endocrine disruption. Exposure to CPF has been shown to induce VTG in male fish (Manjunatha and Philip, 2016), and we have earlier seen altered transcription of genes associated with the Gene Ontology "Response to estrogen stimulus" in Atlantic salmon hepatocytes exposed to CPF (Olsvik et al., 2015). However, no significant effect on *vtg* levels were observed after CPF exposure in this study.

In conclusion, this study shows that CPF exposure leads to reduced levels of several PUFAs and long-chain fatty acids, and mitigate accumulation of MAGs in Atlantic salmon hepatocytes. Supplementation with ARA and EPA could not prevent CPF-induced accumulation of MAGs in the cells, and had only minor impact on other affected lipid species. Most profoundly, co-treatment with PUFAs partly restored the negative effect CPF had on energy metabolism. PUFA supplementation did not counteract CPF-induced oxidative stress.

Supplementary data to this article can be found online at https://doi.org/10.1016/j.tiv.2019.104655.

Declaration of competing interest

The authors declare that they have no known competing financial interests or personal relationships that could have appeared to influence the work reported in this paper.

Acknowledgements

The authors want to thank the Aquarium in Bergen for fish maintenance, and Betty Irgens, Synnøve Winterthun and Eva Mykkeltvedt (Institute for Marine Research) for technical and analytical help. This work was financed by the Nutritox project (The Research Council of Norway, project 200506/I30).

References

Al-Eryani, L., Wahlang, B., Falkner, K.C., Guardiola, J.J., Clair, H.B., Prough, R.A., Cave, M., 2015. Identification of environmental chemicals associated with the development of toxicant-associated fatty liver disease in rodents. Toxicol. Pathol. 43, 482–497.

Almeida, J.R., Oliveira, C., Gravato, C., Guilhermino, L., 2010. Linking behavioural alterations with biomarkers responses in the European seabass *Dicentrarchus labrax* L. exposed to the organophosphate pesticide fenitrothion. Ecotoxicology 19, 1369–1381.

Alvheim, A.R., Torstensen, B.E., Lin, Y.H., Lillefosse, H.H., Lock, E.J., Madsen, L., Hibbeln, J.R., Malde, M.K., 2013. Dietary linoleic acid elevates endogenous 2-arachidonoylglycerol and anandamide in Atlantic salmon (*Salmo salar* L.) and mice, and induces weight gain and inflammation in mice. Brit. J. Nutr. 109, 1508–1517.

Anderson, E.J., Thayne, K.A., Harris, M., Shaikh, S.R., Darden, T.M., Lark, D.S., Williams, J.M., Chitwood, W.R., Kypson, A.P., Rodriguez, E., 2014. Do fish oil omega-3 fatty acids enhance antioxidant capacity and mitochondrial fatty acid oxidation in human atrial myocardium via ppar gamma activation? Antioxid. Redox Signal. 21, 1156–1163.

Basu, P., Burgmayer, S.J., 2011. Pterin chemistry and its relationship to the molybdenum cofactor. Coord. Chem. Rev. 255, 1016–1038.

Cave, M., Falkner, K.C., McClain, A., 2011. Occupational and environmental hepatotoxicity. In: Textbook of Liver Disease (Hepatology). Elsevier Saunders, Philadelphia, pp. 476–492.

Cornet, V., Ouaach, A., Mandiki, S.N.M., Flamion, E., Ferain, A., Van Larebeke, M., Lemaire, B., Lopez, F.E.R., Tort, L., Larondelle, Y., Kestemont, P., 2018. Environmentally-realistic concentration of cadmium combined with polyunsaturated fatty acids enriched diets modulated non-specific immunity in rainbow trout. Aquat. Toxicol. 196, 104–116.

Cranmer-Byng, M.M., Liddle, D.M., De Boer, A.A., Monk, J.M., Robinson, L.E., 2015. Proinflammatory effects of arachidonic acid in a lipopolysaccharide-induced inflammatory microenvironment in 3T3-L1 adipocytes *in vitro*. Appl. Physiol. Nutr. Metab. 40, 142–154.

Darbre, P.D., 2017. Endocrine disruptors and obesity. Curr. Obes. Rep. 6, 18–27.

Du, Z., Zhang, Y., Wang, G., Peng, J., Wang, Z., Gao, S., 2016. TPhP exposure disturbs carbohydrate metabolism, lipid metabolism, and the DNA damage repair system in zebrafish liver. Sci. Rep. 6, 21827.

Ferain, A., Bonnineau, C., Neefs, I., Rees, J.F., Larondelle, Y., De Schamphelaere, K.A.C., Debier, C., 2016. The fatty acid profile of rainbow trout liver cells modulates their tolerance to methylmercury and cadmium. Aquat. Toxicol. 177, 171–181.

Foulds, C., Trevino, L., York, B., Walker, C.L., 2017. Endocrine-disrupting chemicals and fatty liver disease. Nat. Rev. Endocrinol. 13, 445–457.

Ghioni, C., Tocher, D.R., Sargent, J.R., 1997. The effect of culture on morphology, lipid and fatty acid composition, and polyunsaturated fatty acid metabolism of rainbow trout (*Oncorhynchus mykiss*) skin cells. Fish Physiol. Biochem. 16, 499–513.

Grun, F., Blumberg, B., 2007. Perturbed nuclear receptor signaling by environmental obesogens as emerging factors in the obesity crisis. Rev. Endocr. Metab. Disord. 8, 161–171.

Hodgson, E., Rose, R.L., 2008. Metabolic interactions of agrochemicals in humans. Pest Manag. Sci. 64, 617–621.

Inoue-Yamauchi, A., Itagaki, H., Oda, H., 2018. Eicosapentaenoic acid attenuates obesity-related hepatocellular carcinogenesis. Carcinogenesis 39, 28–35.

Ke, N., Wang, X., Xu, X., Abassi, Y.A., 2011. The xCELLigence system for real-time and label-free monitoring of cell viability. Methods Mol. Biol. 740, 33–43.

Liland, N.S., Espe, M., Rosenlund, G., Waagbø, R., Hjelle, J.I., Lie, O., Fontanillas, R., Torstensen, B.E., 2013. High levels of dietary phytosterols affect lipid metabolism and increase liver and plasma TAG in Atlantic salmon (*Salmo salar* L.). Br. J. Nutr. 110, 1958–1967.

Liland, N.S., Hatlen, B., Takle, H., Venegas, C., Espe, M., Torstensen, B.E., Waagbø, R., 2015. Including processed poultry and porcine by-products in diets high in plant ingredients reduced liver TAG in Atlantic salmon, *Salmo salar* L. Aquac. Nutr. 21, 655–669.

Manjunatha, B., Philip, G.H., 2016. Reproductive toxicity of chlorpyrifos tested in zebrafish (*Danio rerio*): histological and hormonal end points. Toxicol. Ind. Health 32, 1808–1816.

Nøstbakken, O.J., Bredal, I.L., Olsvik, P.A., Huang, T.S., Torstensen, B.E., 2012. Effect of marine omega 3 fatty acids on methylmercury-induced toxicity in fish and mammalian cells in vitro. J. Biomed. Biotechnol. 2012 417652.

Oka, T., Nishimura, Y., Zang, L., Hirano, M., Shimada, Y., Wang, Z., Umemoto, N., Kuroyanagi, J., Nishimura, N., Tanaka, T., 2010. Diet-induced obesity in zebrafish shares common pathophysiological pathways with mammalian obesity. BMC Physiol. 10, 21.

Olsvik, P.A., Amlund, H., Torstensen, B.E., 2011. Dietary lipids modulate methylmercury toxicity in Atlantic salmon. Food Chem. Toxicol. 49, 3258–3271.

Olsvik, P.A., Berntssen, M.H.G., Søfteland, L., 2015. Modifying effects of vitamin E on chlorpyrifos toxicity in Atlantic salmon. PLoS One 10, e0119250.

Olsvik, P.A., Berntssen, M.H.G., Søfteland, L., 2017. *In vitro* toxicity of pirimiphos-methyl in Atlantic salmon hepatocytes. Toxicol. in Vitro 39, 1–14.

Olsvik, P.A., Berntssen, M.H.G., Søfteland, L., Sanden, M., 2019a. Transcriptional effects of dietary chlorpyrifos-methyl exposure in Atlantic salmon (*Salmo salar*) brain and liver. Comp. Biochem. Physiol. D 29, 43–54.

Olsvik, P.A., Larsen, A.K., Berntssen, M.G.H., Goksøyr, A., Karlsen, O.A., Yadetie, F., Sanden, M., Kristensen, T., 2019b. Effects of agricultural pesticides in aquafeeds on wild fish feeding on leftover pellets near fish farms. Front. Genet. https://doi.org/10.3389/fgene.2019.00794.

Oruc, E.O., 2010. Oxidative stress, steroid hormone concentrations and acetylcholinesterase activity in *Oreochromis niloticus* exposed to chlorpyrifos. Pestic. Biochem. Physiol. 96, 160–166.

Reddy, J.K., Hashimoto, T., 2001. Peroxisomal beta-oxidation and peroxisome proliferator-activated receptor alpha: an adaptive metabolic system. Annu. Rev. Nutr. 21, 193–230.

Sahini, N., Borlak, J., 2014. Recent insights into the molecular pathophysiology of lipid droplet formation in hepatocytes. Prog. Lipid Res. 54, 86–112.

Sanden, M., Liland, N.S., Saele, O., Rosenlund, G., Du, S.S., Torstensen, B.E., Stubhaug, I., Ruyter, B., Sissener, N.H., 2016. Minor lipid metabolic perturbations in the liver of Atlantic salmon (*Salmo salar* L.) caused by suboptimal dietary content of nutrients from fish oil. Fish Physiol. Biochem. 42, 1463–1480.

Sanden, M., Olsvik, P.A., Søfteland, L., Rasinger, J.D., Rosenlund, G., Garlito, B., Ibanez, M., Berntssen, M.H.G., 2018. Dietary pesticide chlorpyrifos-methyl affects arachidonic acid metabolism including phospholipid remodeling in Atlantic salmon (*Salmo salar* L.). Aquaculture 484, 1–12.

Søfteland, L., Eide, I., Olsvik, P.A., 2009. Factorial design applied for multiple endpoint toxicity evaluation in Atlantic salmon (*Salmo salar* L.) hepatocytes. Toxicol. In Vitro 23, 1455–1464.

Søfteland, L., Kirwan, J.A., Hori, T.S., Størseth, T.R., Sommer, U., Berntssen, M.H., Viant, M.R., Rise, M.L., Waagbø, R., Torstensen, B.E., Booman, M., Olsvik, P.A., 2014. Toxicological effect of single contaminants and contaminant mixtures associated with plant ingredients in novel salmon feeds. Food Chem. Toxicol. 73, 157–174.

Søfteland, L., Berntssen, M.H.G., Kirwan, J.A., Størseth, T.R., Viant, M.R., Torstensen, B.E., Waagbø, R., Olsvik, P.A., 2016. Omega-3 and alpha-tocopherol provide more protection against contaminants in novel feeds for Atlantic salmon (*Salmo salar* L.) than omega-6 and gamma tocopherol. Toxicol. Rep. 3, 211–224.

Staels, B., Rubenstrunk, A., Noel, B., Rigou, G., Delataille, P., Millatt, L.J., Baron, M., Lucas, A., Tailleux, A., Hum, D.W., Ratziu, V., Cariou, B., Hanf, R., 2013. Hepatoprotective effects of the dual peroxisome proliferator-activated receptor alpha/delta agonist, GFT505, in rodent models of nonalcoholic fatty liver disease/nonalcoholic steatohepatitis. Hepatology 58, 1941–1952.

Torstensen, B.E., Espe, M., Stubhaug, I., Lie, O., 2011. Dietary plant proteins and vegetable oil blends increase adiposity and plasma lipids in Atlantic salmon (*Salmo salar* L.). Brit. J. Nutr. 106, 633–647.

Vandesompele, J., De Preter, K., Pattyn, F., Poppe, B., Van Roy, N., De Paepe, A., Speleman, F., 2002. Accurate normalization of real-time quantitative RT-PCR data by geometric averaging of multiple internal control genes. Genome Biol. 3 (7) RESEARCH0034.

Vigor, C., Bertrand-Michel, J., Pinot, E., Oger, C., Vercauteren, J., Le Faouder, P., Galano, J.M., Lee, J.C., Durand, T., 2014. Non-enzymatic lipid oxidation products in biological systems: assessment of the metabolites from polyunsaturated fatty acids. J. Chromatogr. B Anal. Technol. Biomed. Life Sci. 964, 65–78.

Willebrords, J., Pereira, I.V., Maes, M., Crespo Yanguas, S., Colle, I., Van Den Bossche, B., Da Silva, T.C., de Oliveira, C.P., Andraus, W., Alves, V.A., Cogliati, B., Vinken, M., 2015. Strategies, models and biomarkers in experimental non-alcoholic fatty liver disease research. Prog. Lipid Res. 59, 106–125.

Xing, H.J., Li, S., Wang, Z.L., Gao, X.J., Xu, S.W., Wang, X.L., 2012. Oxidative stress response and histopathological changes due to atrazine and chlorpyrifos exposure in common carp. Pestic. Biochem. Physiol. 103, 74–80.

Yamada, S., Kubo, Y., Yamazaki, D., Sekino, Y., Kanda, Y., 2017. Chlorpyrifos inhibits neural induction via Mfn1-mediated mitochondrial dysfunction in human induced pluripotent stem cells. Sci. Rep.-Uk 7.

Zang, L.Q., Maddison, L.A., Chen, W.B., 2018. Zebrafish as a model for obesity and diabetes. Front. Cell Dev. Biol. 6 20 August 2018.

Zechner, R., Zimmermann, R., Eichmann, T.O., Kohlwein, S.D., Haemmerle, G., Lass, A., Madeo, F., 2012. FAT SIGNALS–lipases and lipolysis in lipid metabolism and signaling. Cell Metab. 15, 279–291.